arXiv:1209.0840v1 [cond-mat.quant-gas] 5 Sep 2012

Dynamical excitations in the collision of 2D Bose-Einstein condensates

T. Yang, B. Xiong, and Keith A. Benedict
Theory of Condensed Matter, School of Physics and Astronomy,
University of Nottingham, Nottingham NG7 2RD, United Kingdom

(Dated: September 6, 2012)

Abstract

We carry out simulations of the collision of two components of an adiabatically divided, quasi-2D BEC. We identify under, over and critically damped regimes in the dipole oscillations of the components according to the balance of internal and centre-of-mass (c.m.) energies of the components and investigate the creation of internal excitations. We distinguish the behaviour of this system from previous studies of quasi-1D BEC's. In particular we note that the nature of the internal excitations is only essentially sensitive to an initial phase difference between the components in the overdamped regime.

I. INTRODUCTION

Quantum interference (QI) in atomic BECs has been an important topic since the experiment carried out in Ref.[1] demonstrated the matter-wave nature of condensates. Interference effects have been used to investigate decoherence [2] and vortex production [3, 4] while underpinning many potential applications in metrology, gravitational, temporal and rotational sensing [5–7]. Most experiments on atomic interference have used freely expanding atom clouds [8–10]. An alternative approach, however, involves controlling the the motion of atom clouds using time dependent trapping potentials [11], often generated by atom chips [12], which can be used to study atom-surface interactions and Josephson phenomena[13]. Many discussions of confined-atom interference consider the noninteracting situation [14, 15] or do not address the deleterious effects of interatomic interactions, including dephasing, collisional shifts, and phase diffusion [16–22]. However, in Ref.[23] it was shown that the recombination process of a split condensate is very sensitive to atomic interactions. In this paper we will study the damping of dipole oscillations of colliding, coherent, condensate clouds and the consequent creation of internal excitations in the clouds.

Quasi-2D BEC's can be formed in a highly anisotropic trap of the form

$$\begin{aligned} V_{\text{trap}}(\mathbf{r}) &= V_\perp(x,y) + V_z(z) \\ &= \frac{1}{2}m\omega_\perp^2\left(x^2+y^2\right) + \frac{1}{2}m\omega_z^2 z^2 \qquad , \end{aligned} \tag{1}$$

with $\omega_z \gg \omega_\perp$. In this limit the dependence on the z-coordinate is quenched such that the order parameter has the form $\Psi(x,y,z;t) = \sqrt{N}\phi(x,y;t)e^{-i\omega_z t/2}\exp\{-z^2/2l_z^2\}/(\pi l_z^2)^{1/4}$ where ϕ is normalized to unity. The dynamics of such a 2D BEC is governed by the GP equation

$$i\hbar\partial_t\phi = -\frac{\hbar^2}{2m}\nabla_\perp^2\phi + V_\perp(x,y)\phi + g_2 N\left|\phi\right|^2\phi \qquad , \tag{2}$$

where $g_2 = g_{3D}/\sqrt{2\pi}l_z = 2\sqrt{2\pi}a_s l_z\hbar\omega_z$ is the 2D coupling constant, $l_z = \sqrt{\hbar/m\omega_z}$ is the oscillator length in the tightly confined direction and a_s is the bulk s-wave scattering length.

If a BEC is prepared in such an anisotropic trap by cooling to its ground state and the trap is then suddenly displaced through a distance $-\Delta$ in the x-direction then the cloud will execute simple harmonic motion without any internal distortion. In the absence of interactions the initial state is a simple gaussian which evolves according to

$$\phi(x,y;t) = \phi_0(x - X(t), y)e^{iP(t)x/\hbar} \tag{3}$$

where

$$\phi_0(x,y) = \sqrt{\frac{1}{\pi l_\perp^2}}\exp\{-\left(x^2+y^2\right)/2l_\perp^2\} \qquad , \tag{4}$$

where $l_\perp^2 = \hbar/m\omega_\perp$ and

$$X(t) = \Delta\cos\left(\omega_\perp t\right) \tag{5}$$

$$P(t) = m\omega_\perp\Delta\sin\left(\omega_\perp t\right) \tag{6}$$

which are the position and momentum of a classical particle of mass m prepared at rest at position $x = \Delta$ in the same potential. The inclusion of interactions only alters the form of the initial state, $\phi_0(x,y)$ but does not alter the forms for $X(t)$ and $P(t)$ and, hence, does not qualitatively change the nature of the subsequent dipole oscillation (see section 12.2 of [24]).

We are considering the situation in which a quasi-2D BEC, previously prepared in an anisotropic trap, has been adiabatically divided into two spatially disjoint components while retaining its overall coherence. The two components are supposed to experience slightly different chemical potentials so that they acquire a phase difference proportional to the time, t_h, for which they are held apart: $\theta = \delta\mu\, t$. The trap is then suddenly switched back to a simple parabolic trap. This is equivalent to preparing a BEC in a state that is a superposition of two single clouds (as above) displaced by equal and opposite distances $\pm\Delta$ and with a phase difference, θ

$$\Phi(x,y;t=0) = \frac{1}{\sqrt{2}}\left(\phi_0(x+\Delta,y) + e^{i\theta}\phi_0(x-\Delta,y)\right) \qquad . \tag{7}$$

The system then evolves according to the GP equation. The case of a non-interacting condensate is, of course, exactly solvable as the two components evolve independently. At time $t>0$ the state of the non-interacting system can be written as

$$\Phi(x,y;t) = \frac{1}{\sqrt{2}}\left(e^{-iP(t)x/\hbar}\phi_0(x+X(t),y) + e^{i\theta}e^{iP(t)x/\hbar}\phi_0(x-X(t),y)\right) \tag{8}$$

with $X(t)$ and $P(t)$ as given above. The corresponding density is then

$$n(x,y,z;t) = n_2\left(x,y;t\right)e^{\{-z^2/l_z^2\}}/\sqrt{\pi l_z^2} \tag{9}$$

where

$$\begin{aligned} n_2(x,y;t) &= N\left|\Phi\right|^2 \\ &= \frac{N}{\pi l_\perp^2}e^{-\left(x^2+y^2+X^2(t)\right)/l_\perp^2}\left\{\cosh\left(\frac{2X(t)x}{l_\perp^2}\right) + \cos\left(\frac{2P(t)x}{\hbar} + \frac{\theta}{2}\right)\right\} \qquad . \end{aligned} \tag{10}$$

The two components are maximally overlapped at times $T_n = \left(n+\frac{1}{2}\right)\pi\omega_\perp$ when

$$n(x,y;T_n) = N\frac{1}{\pi l_\perp^2}e^{-\left(x^2+y^2\right)/l_\perp^2}\left\{1 + \cos\left(\frac{2m\omega_\perp\Delta}{\hbar} + \frac{\theta}{2}\right)\right\} \qquad . \tag{11}$$

Corresponding to perfect rectilinear fringes in the x-direction with spacing given by the de Broglie relation $L = h/2m\omega_\perp\Delta$. The initial relative phase difference simply shifts the fringe pattern. As is well known the shot-to-shot reproducibility of the fringe positions is a test of the coherence of the two components.

If we consider the energetics of the non-interacting case we can express the mean-field energy of the initial state as $E_T = E_K + E_P$ where

$$E_K = N\int d^2\mathbf{r}\frac{\hbar^2}{2m}\left|\nabla\phi\right|^2 = N\frac{1}{2m}\left(P(t)\right)^2 + N\frac{1}{2}\hbar\omega_\perp \tag{12}$$

is the kinetic energy and

$$E_P = N \int d^2\mathbf{r} \frac{1}{2} m\omega_\perp^2 \left|\mathbf{r}\right|^2 \left|\phi\right|^2 = N\frac{1}{2} m\omega_\perp^2 \left(X(t)\right)^2 + N\frac{1}{2}\hbar\omega_\perp \tag{13}$$

the (trap) potential energy. We can regroup these into two conserved quantities

$$E_{cm} = N\frac{1}{2} m\omega_\perp^2 \Delta^2 \tag{14}$$

is the energy associated with the bulk motion of the two clouds and

$$E_{\text{int}} = N\hbar\omega_\perp = N\frac{\hbar^2}{ml_\perp^2} \tag{15}$$

is the internal energy of the two clouds (in this case purely the confinement energy).

The inclusion of interactions between the atoms will, naturally modify this picture. While a single BEC, when subject to a displaced trap potential, will execute undamped simple-harmonic motion with no change of shape (dipole mode) a pair of separated components will only only undergo independent dipole oscillations until they spatially overlap. The subsequent dynamics will be more or less complex depending on the relative magnitudes of the centre of mass (c.m.) energy and the mutual interactions.

For moderate interaction strengths we would expect the initial components to be well-described by the Thomas-Fermi approximation

$$\phi_0(x,y) = \begin{cases} \frac{m\omega_\perp^2}{2g_2}\left(R_{TF}^2 - \left|\mathbf{r}\right|^2\right) & \left|\mathbf{r}\right| < R_{TF} \\ 0 & \left|\mathbf{r}\right| > R_{TF} \end{cases} \tag{16}$$

where, as always, R_{TF} is chosen to give the correct total number of particles which yields

$$R_{TF} = \sqrt{2} l_\perp \gamma \tag{17}$$

where the 2D Thomas-Fermi parameter is

$$\gamma = \left(\frac{4Na_s}{l_z\sqrt{2\pi}}\right)^{1/4} \quad . \tag{18}$$

Hence the conserved energy will be $E_T = E_{\text{cm}} + E_{\text{int}}$ where

$$E_{\text{cm}} = N\frac{1}{2} m\omega_\perp^2 \Delta^2 \tag{19}$$

$$E_{\text{int}} = E_{TF} = \frac{2}{3}\mu_{TF} N = N\hbar\omega_\perp\gamma^2 \tag{20}$$

These will not be separately conserved and we expect an irreversible transfer of energy from E_{cm} to E_{int} leading to damping of the dipole oscillations of the two components at the expense of the creation of internal excitations within each cloud.

We seek to define an effective measure of the relative importance of interactions which can be directly evaluated in a simulation. We define a parameter, η_n, at each turning point

$T_n = n\pi/\omega_\perp$ of the dipole oscillation (at which the c.m. kinetic energy is zero) as

$$\eta_n = \frac{E_I}{E_P} = \frac{\frac{1}{2}g_2 \int |\phi(\mathbf{r}, T_n)|^4 \, d^2\mathbf{r}}{\frac{1}{2}m\omega_\perp^2 \int |\mathbf{r}|^2 \, |\phi(\mathbf{r}, T_n)|^2 \, D^2\mathbf{r}} \quad . \tag{21}$$

In the non-interacting limit ($g_2 = 0$) this is identically zero. In the Thomas Fermi régime it will be

$$\eta_n \sim \frac{\hbar\omega_\perp \gamma^2 + \epsilon_{\mathrm{EX}}}{\frac{1}{2}m\omega_\perp^2 \Delta_n^2} \tag{22}$$

where Δ_n is the displacement of the c.m. of the cloud from the centre of the trap at time T_n and ϵ_{EX} is the excitation energy per atom of the cloud (i.e. the excess internal energy of the cloud over the TF energy per particle). Since the scattering will act to damp the dipole oscillations (decreasing Δ) and create excitations within the cloud (increasing ϵ_{EX}) η_n will increase with n.

For low density/weak interactions ($\eta_0 \ll 1$) one expects the two components to undergo underdamped oscillations and to exhibit behaviour which is qualitatively similar to the non-interacting case. In particular we would expect curved fringes while the two clouds are passing through one-another. The scattering processes arising from interactions will produce a frictional force on the cloud tending to reduce its velocity and hence increase the fringe spacing. The frictional force will be largest in the centre of the trap (close to $y = 0$) where the density is highest. In addition, the interaction will lead to an over-pressure in the fringe maxima which will tend to fatten the fringes in the trap centre. At higher densities/stronger interactions we expect to find an overdamped regime in which the two clouds collide and merge into a single cloud containing a variety of excitations seeded by the fringe pattern associated with the opposite pre-collision velocities of the clouds. As we will see it is in this overdamped regime that we observe significant qualitative sensitivity to the initial phase difference, θ, between the two components. A recent experiment [25] showed that the recombination of a split condensate held by an atom chip leads to a heating of the atomic cloud which depends on the relative phase of the two components. This qualitatively agrees with the analytical prediction that the recombination process can lead to exponential growth of unstable modes [23]. This effect, however, is not obvious in the underdamped régime. The rôle of the relative phase can make the dynamics of the interferometer very different in the overdamped régime [25, 26].

In this paper, we present detailed numerical calculations, which now enable us accurately to characterise the behaviour of the interferometer as a function of the distance and the relative phase between the two disk-shaped condensate components. We carry out the simulations in the underdamped, overdamped and critically damped regimes. Our key findings are as follows.

: Underdamped case The cm kinetic energy is much larger than the interatomic interaction energy. In this case the system develops distorted rectilinear fringes.

: Critically damped case The cm kinetic energy and the interatomic interaction energy are of the same order. This means that nonlinearity is important and the effect of scattering becomes noticeable making the dynamics of the system complicated. After the clouds interfere for the first time, topological excitations are created in the system. In both the underdamped and critically damped cases we find that the initial relative phase does not affect the system qualitatively.

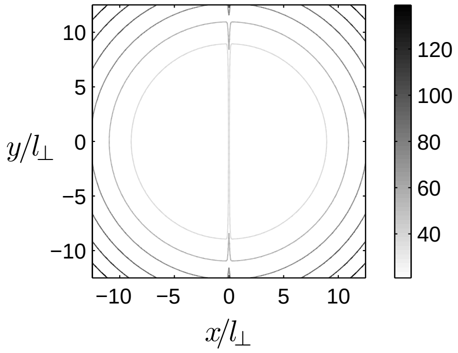

FIG. 1. The equipotential lines of a 2D double well potential with narrow cental barrier along about $x = 0$. The parameters used are $\sigma_x/l_\perp = 0.1$, $\sigma_y/l_\perp = 10$, $U_0/\hbar\omega_\perp = 50$.

: Overdamped case The cm energy is much smaller than the interaction energy, here the system undergoes a merging process and is much more sensitive to the initial relative phase. For zero initial relative phase the two components can merge into a single cloud containing collective excitations, while for a π initial relative phase the merging leads to topological excitations.

II. SYSTEM AND METHODOLOGY

In experiments, a trapped condensate can be split into two components adiabatically, for example by using a tailored magnetic potential from an atom chip [27], by the introduction of an optical barrier via a shaped blue-detuned laser [28] or by passing counterpropagating red-detuned laser beams through an acousto-optic modulator driven at RF frequency [25] to form a double well potential in the horizontal plane. The two components of the split condensate are held in an asymmetric double well potential for varying hold times to set the relative phase between them. The recombination of the two components after splitting can be realised by reducing the RF frequency for variable recombination times.

We based our simulations on a condensate of $N = 2 \times 10^4\ {}^{87}R_b$ atoms in a trap potential with $\omega_\perp = 2\pi \times 5H_z$ and $\omega_z = 2\pi \times 100H_z$. To simulate the underdamped and critically damped cases, we obtained the configuration, $\phi_0(x, y)$, of the order parameter which minimised the mean field energy subject to the constraint $\int d^2\mathbf{r}\, |\phi_0|^2 = 1$. The initial state for the simulations was then

$$\Phi(x, y; t = 0) = \frac{1}{\sqrt{2}} \left(\phi_0(x + \Delta, y) + e^{i\theta}\phi_0(x - \Delta, y)\right) \qquad . \tag{23}$$

The order parameter was then allowed to evolve in the quasi-2D trap potential. To reach the overdamped regime required $\Delta < R_{\mathrm{TF}}$ so another method of preparing the initial state

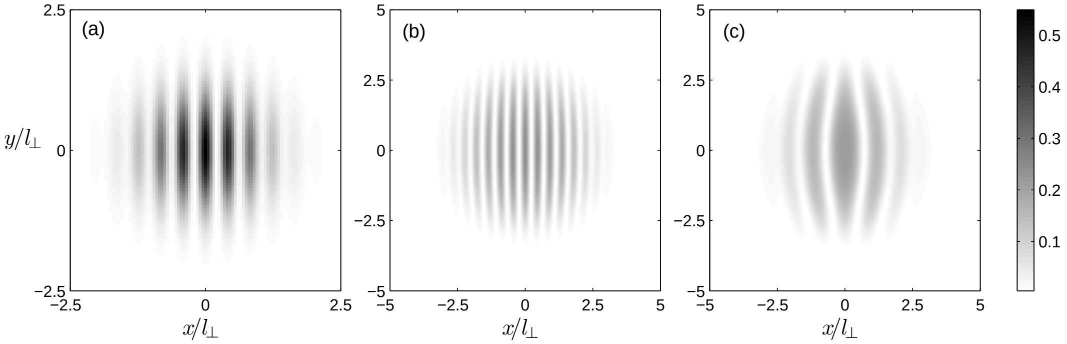

FIG. 2. Normalised density profiles of the two condensate components without initial phase difference colliding at the bottom of the trap. (a) noninteracting case with $\Delta = 7.5 l_\perp$; (b) interacting case with $\Delta = 7.5 l_\perp$; (c) interacting case with $\Delta = 4 l_\perp$.

was used. The lowest energy configuration of the order parameter was found in a potential

$$V_{DW}(x, y) = \frac{1}{2} m\omega_\perp^2 (x^2 + y^2) + U_0 e^{-\frac{x^2}{\sigma_x^2} - \frac{y^2}{\sigma_y^2}}. \tag{24}$$

where the second term represents the effect of a narrowly focussed, blue-detuned laser applied to split the condensate. The height of the central barrier is given by the amplitude of the Gaussian function U_0, and the distance between the two wells can be adjusted using the parameters σ_x and σ_y. We can see two distinct potential minima clearly in Fig. 1, which have the same shape as the RF-induced potential in the experiment in Ref.[29]. The phase difference between the two parts can be achieved by using phase imprinting method [30] in experiments. The parameters we used in our simulations are $\sigma_x/l_\perp = 0.1$, $\sigma_y/l_\perp = 10$, and $U_0/\hbar\omega_\perp = 50$. We then used this configuration as the initial state for real-time evolution of the GP equation, representing the sudden removal of the laser.

In our discussion we will always keep the interaction strength and the number of atoms in the system fixed. The only quantities we change are the initial displacement and the initial relative phase of the condensate components. The ground state wave function of the condensate is obtained by the imaginary-time-evolution method [31] for the time-dependent GP equation (2). We use a reduced scattering length for ^{87}Rb, $a_s = 0.3 \times 5.4 nm$ to see the structure of vortex excitation clearly in our simulation. To consider the effect of the relative phase on the dynamics, we keep the initial phase of one component fixed and adjust the initial phase of the other from 0 to 2π.

III. NUMERICAL SOLUTION AND RESULTS

In the numerical investigations we used $l_\perp$ as the unit of length and $1/\omega_\perp$ as the unit of time. Hence we define dimensionless wavevectors $\tilde{k} = k l_\perp$, times $\tilde{t} = \omega_\perp t$ and frequencies $\tilde{\omega} = \omega/\omega_\perp$.

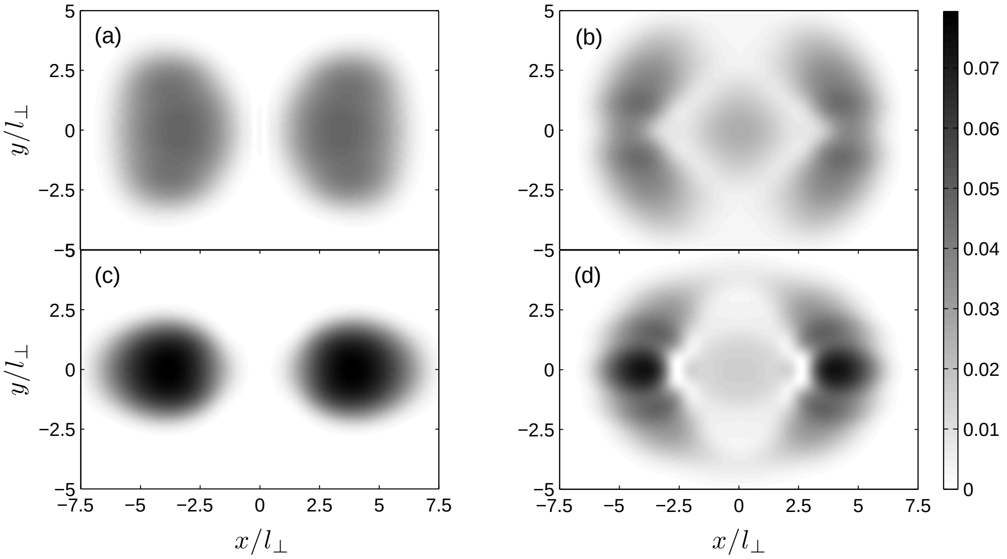

FIG. 3. Normalised density profiles of the colliding components in the trap without initial phase difference. The initial separation Δ is $7.5l_\perp$ (a)(c) and $4l_\perp$ (b)(d) respectively. Times are (a) $\tilde{t} = 2.15$, (b) $\tilde{t} = 3.05$ and (c)$\tilde{t} = 4.25$, (d) $\tilde{t} = 3.5$.

A. Scattering effect in the underdamped régime

As we have discussed, the importance of the scattering between atoms depends on the competition between the cloud kinetic energy and the interaction energy, which in turn affect the dynamics of the system.

In Fig. 2, we show the density profiles at the point of maximum overlap ($\tilde{t} = \pi/2$) of the two components with zero initial phase difference starting from different displacement positions. The bright region is a low density area, while the dark region is a high density area. For a noninteracting system there is only kinetic energy so $\eta = 0$. In this linear regime the unperturbed condensates always show straight fringes during the interference as seen in Fig. 2(a). For interacting systems when the displacement is large, the clouds will have maximum c.m. kinetic energy, i.e. high relative peak velocity when they begin to interfere. The system still responds linearly. The duration of the collision is correspondingly short and the effect of scattering is very small. In Fig. 2(b), the initial separation is set to be $\Delta = 7.5l_\perp$. We can see that interference fringes are nearly straight. With smaller initial separations, the components reach a smaller peak velocity, the interaction energy is comparable to the kinetic energy and the duration of the collision is correspondingly longer. As is shown in Fig. 2(c), where $\Delta = 4l_\perp$, the distortion of the fringes has become quite sizable. The width of the fringes increases with the nonlinearity, while the peak density does not change dramatically in comparison to that of the fringes in the linear situation (Fig. 2(b)). The nonlinear situation however gives us fewer fringes associated with the damping of the dipole oscillation of each cloud. The expansion rate of the central fringe is highly nonuniform along y-axis due to the non-uniform density distribution. At the centre of the clouds, where the density is highest, the fringes expand most. The spacing of fringes are close to their non-interacting value towards the edge of the cloud (low density region) where the interaction is negligible. This leads to the central fringe taking a lenticular shape, accompanied by the bending of the other fringes. There is only the central fringe left eventually before the two

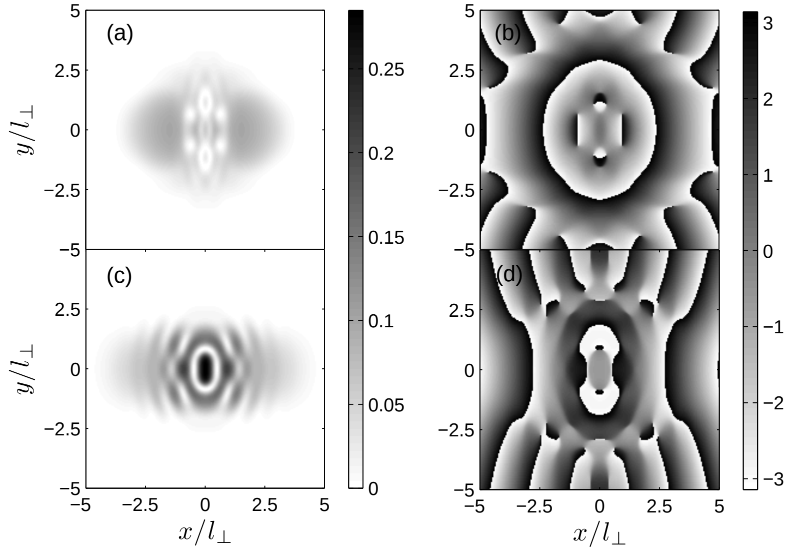

FIG. 4. The normalised density profiles (the left panels) and the corresponding phase plots (the right panels) of the colliding condensate components in a trap during the second recombination. This is the continuation of the simulation shown in Fig. 3. From (a) and (b) we can see clearly the formation of two vortex pairs located at the left and the right side of the centre of the trap. curved solitons arise in the centre of the trap. These vortex pairs approach each other until the vortices with opposite charges annihilate, forming a soliton ring as seen in (c) and (d). The vortex ring will decay into vortices thereafter. Times are (a,b) $\tilde{t} = 4.15$, (c,d) $\tilde{t} = 4.5$.

components start to separate.

In Fig. 3 we show the density profiles of the two components without initial phase difference after their first collision, where the initial separation Δ is $7.5l_\perp$ (a)(c) and $4l_\perp$ (b)(d) respectively. The effect of interactions is not obvious in the linear regime ($\Delta = 7.5l_\perp$). As seen in Fig. 3(a) the condensate expands a little bit in the y-direction which means that some atoms gain a y-component to their momentum via scattering. This momentum is small, however, due to the short collision time, which means that the scattering induced distortion of condensates is not obvious after the first collision. After the first collision the clouds pass through each other; each moving towards the original position of the other. The density profile of the condensate will vary in a manner similar to the the breathing mode and the components will undergo a damped c.m. oscillation. Fig. 3(c) shows that the clouds regain their original shape with a small distortion at $\tilde{t} = 4.25$ before their second collision.

When the initial separation is reduced, the maximum c.m. kinetic energy is correspondingly smaller and the nonlinear interaction term in Eq.(2) becomes more important. We reach the critically damped regime (e.g., $\Delta = 4l_\perp$) where the cloud energy is comparable to the interaction energy. As seen in Fig. 3(b) the modulation of the density in the middle of the component (high density area) moves rapidly in the y-direction due to strong scattering, leading to two density peaks appearing symmetrically about the x-axis for each component (see Fig. 3(b)). Due to the trap potential, self-interference occurs when these two density maxima move back towards one other as seen in Fig. 3(d). The most distinct feature in this regime is that the clouds no longer pass cleanly through each other and regain their original shape after their collision. We can see clearly that there are more structures in

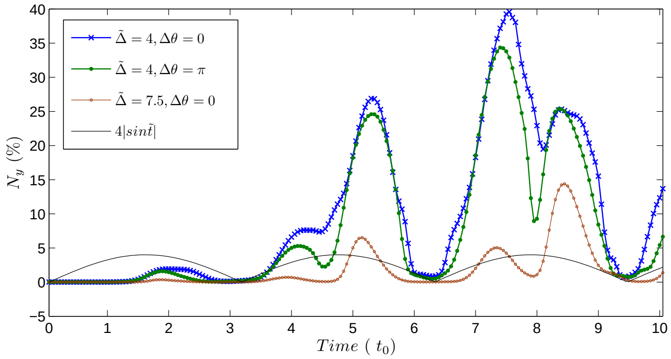

FIG. 5. Oscillations of condensate atom number N_y for different initial conditions.

the condensate in Fig. 3(d) than in Fig. 3(c). The interference fringes will be completely distorted when the second collision begins and this leads to excitations in the form of vortex pairs and soliton rings as shown in Fig. 4.

In Fig. 5, we show quantitatively the scattering effect by plotting the dynamics of N_y, which is the number of atoms with y-component of momentum $|\tilde{k}_y| > 10d\tilde{k}$ where $2\pi/\tilde{k}$ is the spatial resolution of the simulation. As seen in the figure, the initial value of $\tilde{k}_y$ is 0 because the condensate components are set to move along the x-axis. The black solid line is the absolute value of a sinusoidal curve fitted with fixed frequency $\tilde{\omega} = 1$ which indicated that there are two collisions during one dipole period. For all three distinct initial conditions there is only one peak during the first half period because the scattering occurs after the two components collide at the bottom of the trap ($\tilde{t} \sim \pi/2$). The peak value increases with decreasing Δ. After the first half period two peaks appear. The first one is induced by the self-interference in the y-direction of each component, and the second one arises from the collision of the two components. For the underdamped case (the line marked with open circles) the self-interference induced scattering is always weaker than the collision induced scattering before the conditions of the linear regime are violated (recall that η_n increases with n), while it is true for the critically damped case (the line marked with cross and the line marked with dot) only in the second half period. In this intermediate regime the creation of solitons and vortices after the second half period suppress the scattering along the x-direction (collision induced scattering), which makes the second peak lower than the first one.

Generally in the above regimes the initial phase difference of two components will not change the physics intrinsically. Especially for the underdamped situation, only the location of the fringes varies with the relative phase $\Delta\theta$, while the period and spacing of the fringes are not changed. In the underdamped regime, the trajectory is independent of $\Delta\theta$ indicating that the initial relative phase will not change the scattering properties at all. In the critically damped regime the only difference between the $\Delta\theta = 0$ (dotted line) and $\Delta\theta = \pi$ trajectories is the peak values. An interesting point is that the peak values of $\Delta\theta = \pi$ is always smaller than those of $\Delta\theta = 0$, which is different from the results for the merging process (overdamped collision) in Ref.[32] where the atom loss after recombination increased as the relative phase increased from 0 to π.

If we reduce the distance between two components further, the interaction energy will

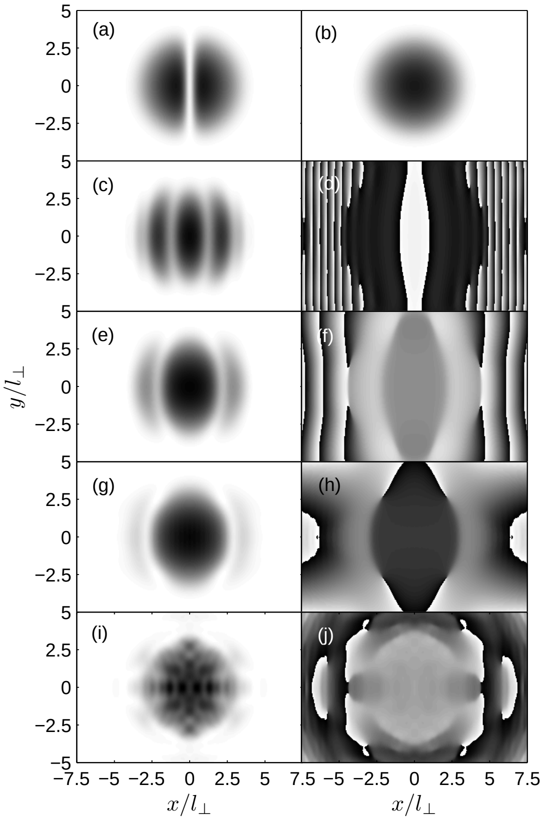

FIG. 6. The normalised density profiles and phase plots of the condensates prepared in a double well potential which are released into a harmonic potential well at time $t = 0$. The initial relative phase is $\Delta\theta = 0$. The left panels are the density profiles of the condensates prepared in a double well potential (a) and then released in the harmonic potential (c, e, g, i). (d, f, h, j) are the corresponding phase plots of (c, e, g, i) respectively. (b) is the density profile of the ground state condensate with $2N$ atoms in the harmonic potential well. The density profile of the dynamic state (g) is close to the ground state (b), but with some distortion and a few excited atoms around it. Density and phase modulations are obvious in plots (e) and (j). Times are (a) $\tilde{t} = 0$, (c, d) $\tilde{t} = 0.5$, (e,f) $\tilde{t} = 1.0$, (g, h) $\tilde{t} = 1.57$, (i, j) $\tilde{t} = 10$.

dominate the system. In this overdamped situation the dynamics of the system could be very different from the cases we have considered so far. The two components could merge into one condensate after the first collision. In the next section we will look at this nonlinear regime where the initial relative phase plays a more important role.

B. Phase-sensitivity of excitations in overdamped collisions

In Ref.[25, 26], it was reported that for elongated components that are tightly confined in the radial directions, when the central barrier potential is suddenly turned off, two components merge into a single cloud. When the initial relative phase between the two components

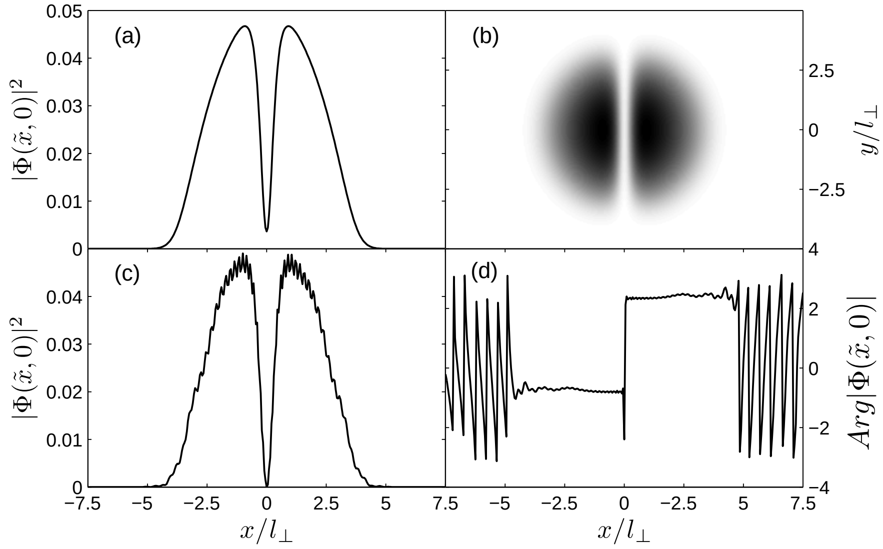

FIG. 7. (a) The initial density profile of a condensate prepared in a 2D double well potential at $y = 0$. (b) the top view of the initial density profile. Density (c) and phase (d) profile at $\tilde{t} = 0.5$ and $y = 0$.

is zero, the merged cloud is in its ground state with respect to the trapping potential. When the initial relative phase is π, the merged condensate contains a dark soliton.

For 2D disk-shaped clouds, the size of the condensate in the merging direction (x-axis in our case) is large. As we have seen, when the separation between the c.m. of the two components is comparable to the diameter of one cloud, i.e. $\Delta \sim R_{TF}$, the cloud kinetic energy that the components will have is comparable to the interaction energy. This energy is high enough to prevent the two components merging into one condensate after the first collision, as they will not lose sufficient momentum in the merging direction due to scattering. If we want to investigate the merging of 2D condensate components we need to enter the overdamped regime where the interaction energy dominates the system, i.e. $\Delta < R_{TF}$. This means that there will be an overlap between the two components which depends on the height and width of the central barrier of the trap, V_{DW} (see equation 24).

As we have seen, solitons are created during the interference process. We know that soliton stability depends on the nonlinearity and geometry of the medium [33]. In general, solitons in BECs are always thermodynamically unstable, and dark solitons in BECs are also expected to be inherently dynamically unstable [34–37]. The velocity of a soliton v_s is [38]

$$v_s/v_c = cos(\Delta\theta/2) = [1 - n_d/n]^{1/2}. \tag{25}$$

$v_c = (g_{2D}n/m)^{1/2}$ is the speed of sound, $n = |\phi_0|^2$ is the unperturbed condensate density, and n_d is the difference between n and the minimum density in the centre of the soliton. For a given density, increasing the relative phase from 0 to π will decrease the velocity of the dark soliton. The two limiting cases are $\theta = 0$ and $\theta = \pi$, where the velocity of a soliton is v_c and 0 respectively. The formation of vortex pairs inside the combined condensate depends strongly on the velocity of the soliton v_s and the density distribution of condensates.

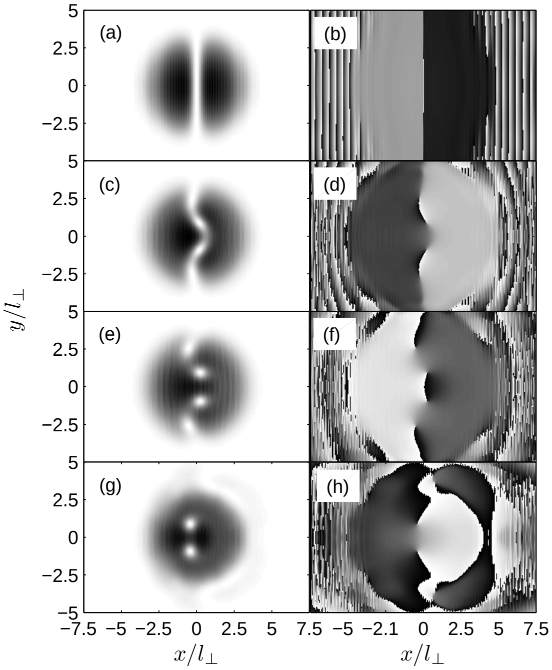

FIG. 8. Sequence showing density profiles (left panels) and the corresponding phase diagrams (right panels) for components prepared in a double well potential undergoing a sudden merger in a harmonic trap. The initial relative phase is $\Delta\theta = \pi$. Times are (a,b) $\tilde{t} = 0.5$, (c,d) $\tilde{t} = 7.5$, (e,f) $\tilde{t} = 8$, (g,h) $\tilde{t} = 15.2$.

Firstly, we consider the situation for which the initial relative phase between the components is 0. As shown in Fig. 6(a), there is an overlap between the components in the left well and that in the right well. The dynamics of the two components will lead to them interfering and merging after the central barrier is turned off. The spacing of the central fringe increases with time until the two components reach their maximum overlap and the shape of the central fringe is close to that of the ground state of a condensate with $2N$ atoms in the harmonic trap (see Fig. 6(g) and (b)). The outer fringes nearly vanish and the two components merge into one with some excited atoms being found near the edge of the cloud (see Fig. 6(g)). The scattering is sufficient due to the long collision time which ensures that the combined condensate can not separate any more. The expansion of the condensate is not as obvious as in Fig. 3(b) due to the small maximum c.m. kinetic energy of the components and the fact that the interatomic interaction dominates the system. However the cloud cannot reach its ground state, as would happen in the 1D case, because the trapping frequency in the merging direction is too low. As predicted by Eq.25 the dark solitons move at v_c and decay rapidly so the system should be dominated by density wave excitations. In Fig. 6(g)(h) we see that a state with density and phase modulations, but without topological defects, is obtained, meaning the system is in a collective excited mode.

Secondly, we consider the situation where the initial relative phase is π, but with the other conditions are kept unchanged. We find this merging process is completely different

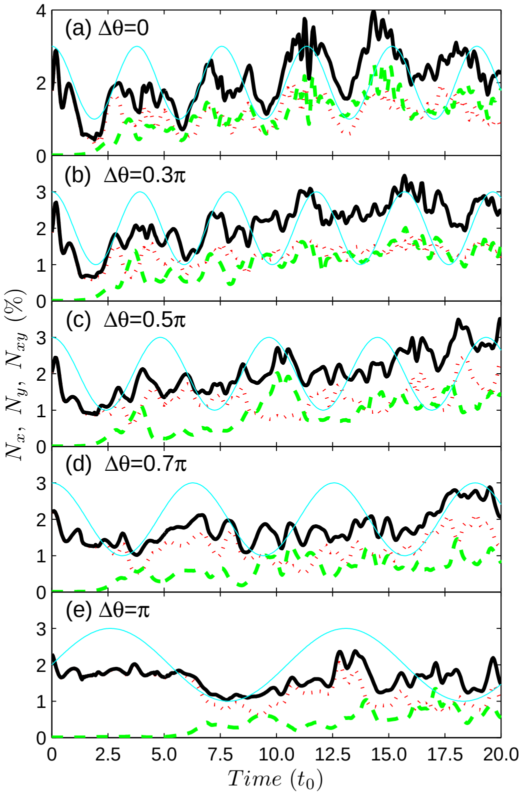

FIG. 9. Oscillations of condensate atom number N_x (red dotted line), N_y (green dashed line) and N_{xy} (thick solid line) for different initial relative phases. The cyan thin lines are sinusoidal curves fitted with frequencies $\tilde{\omega} = 1.66$ (a), 1.6 (b), 1.3 (c), 1.0 (d), 0.6 (e).

to the case where $\Delta\theta = 0$, and that it is also distinct from the 1D merging of condensates with relative phase π reported by Ref.[25] and Ref.[26], where the merging time is too fast (merging occurs in the tight confining direction) to make the soliton decay. In 2D cases the radial frequency of the trap is weak, and so will not quench mechanical excitations in either x- or y-direction. As seen in Fig. 7(a) and (b), the condensates with relative phase π are initially prepared in a double well potential. At time $t = 0$, the central gaussian barrier is turned off suddenly. For interference with π relative phase there should be two central fringes. Due to the small initial separation of the two components, these two central fringes are very fat and nearly keep the original shape of the initial clouds. Our simulations show that two density waves propagate in opposite directions at a reduced amplitude as seen in Fig. 7(c). The initial soliton will eventually reach a point where its central density is zero (see Fig. 7(c) and (d)), and the phase difference is π between the two parts, where a completely dark soliton (black soliton) is created. The velocity of the black soliton is zero. In Fig. 8, we give the snapshots of the time evolution of the condensates which show that the black soliton is not as stable as in the merging of elongated components. After approximately 143ms ($\tilde{t} \simeq 4.5$) of real-time propagation, the black soliton begins to undulate. It is bent at first, then divides into two from the middle with atoms passing through the centre and propagating from left to right. The atoms in the right cloud are pushed by these additional atoms and then two paths from right to left are formed, one above and one below the centre of the cloud, leading to the decay of the solitons via the snake instability [39, 40]. A pair of vortices form near the centre of the condensate and subsequently the other two vortices nucleate at the edge of the cloud, move around the edge to the left and towards each other, and then annihilate at $y = 0$. We note that due to the initial π relative phase the two components are still distinguishable by the phase difference as shown in Fig. 8(f) and (h).

For initial relative phases between 0 and π, the initial dark soliton propagates in the positive x direction, and curves with the expansion of the central interference fringe. This curvature is similar to that observed in Ref.[38]. However the dark soliton will eventually decay into vortex pairs instead of oscillating in the trap.

The nonuniform density distribution in our system makes the speed of a soliton a function of y, which leads to the curvature of the solitons. the formation of vortex pairs inside the combined condensate would require longer lifetimes (i.e. smaller velocity) for the solitons. In Fig. 9 N_x is the number of atoms with $\left|\tilde{k_x}\right| > 10d\tilde{k}$, and N_{xy} is the number of atoms with $\left|\tilde{k_x}\right|$ and $\left|\tilde{k_y}\right|$ larger than $10d\tilde{k}$. We can see that N_y is almost unchanged until the soliton began to decay (green dashed line), which means that the scattering in the $y-$direction is suppressed by the formation of solitons. The lifetime of solitons increases as $\Delta\theta$ is increased from 0 to 2π as predicted by Eq.25. When $\Delta\theta$ is smaller than $\pi/2$ the oscillation frequencies of N_x and N_y are nearly the same after the decay of solitons as is that of the N_{xy} oscillation. When $\Delta\theta = 0$ the velocities of the accompanying density waves are close to v_c [41] and the corresponding frequencies are close to $2\omega_\perp$. As shown in Fig. 9(d) and (e), when $\Delta\theta$ is above $\pi/2$ the formation of vortices inside the combined condensate as seen in Fig. 8 (g) will diminish the amplitude of the number oscillation, which means that the presence of vortex pairs in the combined condensate suppresses density waves.

IV. CONCLUSION

In this paper we have discussed the excitations created when a quasi 2D BEC is first divided into two coherent components and which are then driven to collide by a harmonic potential. The collision and merging processes are quite different to those in 1D or quasi-1D (elongated) systems. However the fact that the dynamical excitations depend not only on the initial separation of the components but also on their initial relative phase is the same as the 1D case reported in Ref.[25, 26]. Generally the dynamics of the system are decided by the competition between the c.m. energy and the internal energy of the colliding components, but it is not simply that the smaller is the maximal c.m. kinetic energy, the easier it is to excite vortices in a system of interfering BECs. When the kinetic energy dominates, the scattering is less effective due to the short collision time and linear interference is observed. There are no dynamical excitations after the two components are separated and the excitation properties are not phase sensitive. If the maximal c.m. kinetic energy is comparable to the interaction energy, the scattering is effective which makes the transverse self-interference of each component obvious. The combination of the interferences in both $x-$ and $y-$direction makes the dynamical excitations in the system quite complicated. However the role of initial phase difference is still limited to the position of fringes. When the interaction energy is much larger than the kinetic energy (merging process) the scattering is still less effective because of the small maximum c.m. kinetic energy of the components and the longer lifetime of solitons. N_{xy} is smaller than 4% during our simulations. The two components can merge into one in this case. The final states are, however, excited in different ways, depending on the initial relative phase. We found that, only when the initial relative phase is larger than $\pi/2$, will there be a vortex pair which can persist in the combined condensate. Otherwise, all the vortex pairs formed in the merging process will only move around the edge of the combined condensate and escape so that the system is left with density wave excitations. The formation of vortices inside the condensate suppress the density wave oscillations.

ACKNOWLEDGMENTS

This work was supported by the EPSRC.We would like to thank Mark Fromhold and Andrew Henning for many useful discussions.

[1] M. R. Andrews, D. M. Kurn, H.-J. Miesner, D. S. Durfee, C. G. Townsend, S. Inouye, and W. Ketterle, Phys. Rev. Lett. **79**, 553 (1997).

[2] Hugbart, M., J. A. Retter, F. Gerbier, A. F. Veron, S. Richard, J. H. Thywissen, D. Clement, P. Bouyer, and A. Aspect, Eur. Phys. J. D **35**, 155 (2005).

[3] E. L. Bolda and D. F. Walls, Phys. Rev. Lett. **81**, 5477 (1998).

[4] F. Chevy, K. W. Madison, V. Bretin, and J. Dalibard, Phys. Rev. A **64**, 031601 (2001).

[5] T. L. Gustavson, P. Bouyer, and M. A. Kasevich, Phys. Rev. Lett. **78**, 2046 (1997).

[6] S. Gupta, K. Dieckmann, Z. Hadzibabic, and D. E. Pritchard, Phys. Rev. Lett. **89**, 140401 (2002).

[7] Y.-J. Wang, D. Z. Anderson, V. M. Bright, E. A. Cornell, Q. Diot, T. Kishimoto, M. Prentiss, R. A. Saravanan, S. R. Segal, and S. Wu, Phys. Rev. Lett. **94**, 090405 (2005).

[8] D.W. Keith, C. R. Ekstrom, Q. A. Turchette, and D. E. Pritchard, Phys. Rev. Lett. **66**, 2693 (1991).

[9] M. Kasevich and S. Chu, Phys. Rev. Lett. **67**, 181 (1991).

[10] P. Berman, *Atom Interferometry* (Academic, New York, 1997).

[11] Y. Shin, M. Saba, T. A. Pasquini, W. Ketterle, D. E. Pritchard, and A. E. Leanhardt, Phys. Rev. Lett. **92**, 050405 (2004).

[12] J. Fortágh and C. Zimmermann, Rev. Mod. Phys. **79**, 235 (2007).

[13] M. Albiez, R. Gati, J. Fölling, S. Hunsmann, M. Cristiani, and M. K. Oberthaler, Phys. Rev. Lett. **95**, 010402 (2005).

[14] W. Hänsel, J. Reichel, P. Hommelhoff, and T. W. Hänsch, Phys. Rev. A **64**, 063607 (2001).

[15] E. Andersson, T. Calarco, R. Folman, M. Andersson, B. Hessmo, and J. Schmiedmayer, Phys. Rev. Lett. **88**, 100401 (2002).

[16] W. Hänsel, J. Reichel, P. Hommelhoff, and T. W. Hänsch, Phys. Rev. A **64**, 063607 (2001).

[17] E. Andersson, T. Calarco, R. Folman, M. Andersson, B. Hessmo, and J. Schmiedmayer, Phys. Rev. Lett. **88**, 100401 (2002).

[18] M. Lewenstein and L. You, Phys. Rev. Lett. **77**, 3489 (1996).

[19] E. M. Wright, D. F. Walls, and J. C. Garrison, Phys. Rev. Lett. **77**, 2158 (1996).

[20] J. Javanainen and M. Wilkens, Phys. Rev. Lett. **78**, 4675 (1997).

[21] A. J. Leggett and F. Sols, Phys. Rev. Lett. **81**, 1344 (1998).

[22] J. Javanainen and M. Wilkens, Phys. Rev. Lett. **81**, 1345 (1998).

[23] J. A. Stickney and A. A. Zozulya, Phys. Rev. A **68**, 013611 (2003).

[24] L. Pitaevskii and S. Stringari, *Bose-Einstein Condensation* (Oxford Science Publications, Oxford, 2003).

[25] G.-B. Jo, J.-H. Choi, C. A. Christensen, T. A. Pasquini, Y.-R. Lee, W. Ketterle, and D. E. Pritchard, Phys. Rev. Lett. **98**, 180401 (2007).

[26] R. G. Scott, D. A. W. Hutchinson, T. E. Judd, and T. M. Fromhold, Phys. Rev. A **79**, 063624 (2009).

[27] Y. Shin, C. Sanner, G.-B. Jo, T. A. Pasquini, M. Saba, W. Ketterle, D. E. Pritchard, M. Vengalattore, and M. Prentiss, Phys. Rev. A **72**, 021604 (2005).

[28] D. R. Scherer, C. N. Weiler, T. W. Neely, and B. P. Anderson, Phys. Rev. Lett. **98**, 110402 (2007).

[29] T. Schumm, P. Krger, S. Hofferberth, I. Lesanovsky, S. Wildermuth, S. Groth, I. Bar-Joseph, L. M. Andersson, and J. Schmiedmayer, Quantum Information Processing **5**, 537 (2006).

[30] L. Dobrek, M. Gajda, M. Lewenstein, K. Sengstock, G. Birkl, and W. Ertmer, Phys. Rev. A **60**, R3381 (1999).

[31] M. L. Chiofalo, S. Succi, and M. P. Tosi, Phys. Rev. E **62**, 7438 (2000).

[32] G.-B. Jo, J.-H. Choi, C. A. Christensen, T. A. Pasquini, Y.-R. Lee, W. Ketterle, and D. E. Pritchard, Phys. Rev. Lett. **98**, 180401 (2007).

[33] Y. S. Kivshar and B. Luther-Davies, Physics Reports **298**, 81 (1998).

[34] L. D. Carr, M. A. Leung, and W. P. Reinhardt, J. Phys. B **33**, 3983 (2000).

[35] D. L. Feder, M. S. Pindzola, L. A. Collins, B. I. Schneider, and C. W. Clark, Phys. Rev. A **62**, 053606 (2000).

[36] A. E. Muryshev, H. B. van Linden van den Heuvell, and G. V. Shlyapnikov, Phys. Rev. A **60**, R2665 (1999).

[37] P. O. Fedichev, A. E. Muryshev, and G. V. Shlyapnikov, Phys. Rev. A **60**, 3220 (1999).

[38] J. Denschlag, J. E. Simsarian, D. L. Feder, C. W. Clark, L. A. Collins, J. Cubizolles, L. Deng, E. W. Hagley, K. Helmerson, W. P. Reinhardt, S. L. Rolston, B. I. Schneider, and W. D. Phillips, Science **287**, 97 (2000).

[39] A. V. Mamaev, M. Saffman, and A. A. Zozulya, Phys. Rev. Lett. **76**, 2262 (1996).

[40] A. V. Mamaev, M. Saffman, D. Z. Anderson, and A. A. Zozulya, Phys. Rev. A **54**, 870 (1996).

[41] S. Burger, K. Bongs, S. Dettmer, W. Ertmer, K. Sengstock, A. Sanpera, G. V. Shlyapnikov, and M. Lewenstein, Phys. Rev. Lett. **83**, 5198 (1999).